参考文献

1) Nath R, Anderson LL, Meli JA, et al. Code of practice for brachytherapy physics: Report of the AAPM Radiation Therapy Committee Task Group No. 56. American Association of Physicists in Medicine. Med Phys 1997; 24(10): 1557-1598.
2) Yu Y, Anderson LL, Li z, et al. Permanent prostate seed implant brachytherapy: Report of the American Association of Physicists in Medicine. Task Group No. 64. Med Phys 1999; 26(10): 2054-2076.
3) 山下 孝, 高橋 豊, 陽田伊織, 他. I-125永久挿入治療物理QAガイドライン. 2008. (In Press)
4) Nath R, Anderson LL, Luxton G, et al. Dosimetry of interstitial brachytherapy sources: Recommendations of the AAPM Radiation Therapy Committee Task Group No. 43. American Association of Physicists in Medicine. Med Phys 1995; 22(2): 209-234.
5) Rivard MJ, Coursey BM, DeWerd LA, et al. Update of AAPM Task Group No. 43 Report: A revised AAPM protocol for brachytherapy dose calculations. Med Phys 2004; 31(3): 633-674.
6) Arsenault C, Bissonnette J, Dunscombe P, et al. Standards for quality control at Canadian Radiation Treatment Centers: Canadian Association of Provincial Cancer Agencies, 2005.
7) Bidmead M, Briot E, Burger J, et al. A Practical Guide to Quality Control of Brachytherapy Equipment. ESTRO Booklet No. 8, 2004.
8) Kubo HD, Coursey BM, Hanson WF, et al. Report of the Ad hoc committee of the AAPM radiation therapy Committee on ^{125}I sealed source dosimetry. Int J Radiat Oncol Biol Phys 1998; 40(3): 697-702.
9) Williamson JF, Nath R. Clinical implementation of AAPM Task Group 32 recommendations on brachytherapy source strength specification. Med Phys 1991; 18: 439-448.
10) Wallner K, Roy J, Harrison L. Dosimetry guidelines to minimize urethral and rectal morbidity following transperineal I-125 prostate brachytherapy. Int J Radiat Oncol Biol Phys 1995; 32(2): 465-471.
11) Takahashi Y, Ito A, Sumida I, et al. Dosimetric consideration of individual ^{125}I source strength measurement and a large-scale comparison of that measured with a nominal value in permanent prostate implant brachytherapy. Radiat Med 2006; 24(10): 675-679.

DISEASES OF THE COLON & RECTUM

ORIGINAL CONTRIBUTION

Preoperative Radiation Response Evaluated by 18-Fluorodeoxyglucose Positron Emission Tomography Predicts Survival in Locally Advanced Rectal Cancer

Keiichi Nakagawa, M.D.[1] • Hideomi Yamashita, M.D.[1] • Naoki Nakamura, M.D.[1] • Hiroshi Igaki, M.D.[1] • Masao Tago, M.D.[1] • Yoshio Hosoi, M.D.[2] • Toshimitsu Momose, M.D.[1] • Kuni Ohtomo, M.D.[1] • Tetsuichiro Muto, M.D.[3] • Hirokazu Nagawa, M.D.[2]

1 Department of Radiology, University of Tokyo Hospital, Tokyo, Japan
2 Department of Surgical Oncology, University of Tokyo Hospital, Tokyo, Japan
3 Department of Surgical Oncology, The Cancer Institute Hospital, Tokyo, Japan

PURPOSE: This study focuses on the prognostic survival value of postirradiation metabolic activity in primary rectal cancer as measured with 18-fluorodeoxyglucose positron emission tomography.

METHODS: From July 1995 to March 2002, all 59 patients underwent two series of fluorodeoxyglucose positron emission tomography: one before preoperative radiation (standardized uptake values-1), and the other two to three weeks after radiation (standardized uptake values-2). Standardized uptake values-1 and standardized uptake values-2 correspond to before and after radiation, respectively.

RESULTS: In univariate analysis, the following emerged as significant prognostic variables: with or without residual tumor, pathologic differentiation, with or without recurrence, standardized uptake values-2, and with or without lymph node metastases. In multivariate analysis, residual tumor and standardized uptake values-2 were significant prognostic factors for survival. The median survival and the five-year overall survival rate comparing standardized uptake values-2 values <5 *vs.* >5 were 95 *vs.* 42 months and 70 *vs.* 44 percent, respectively ($P=0.042$).

CONCLUSION: A significant survival benefit was observed in patients with low fluorodeoxyglucose uptake after preoperative radiotherapy in primary tumors of rectal cancer.

KEY WORDS: Positron emission tomography; Radiotherapy; Prognostic value; Standardized uptake values; Rectal cancer; Preoperative radiation.

A number of studies have reported that preoperative radiotherapy (RT) reduces the recurrence rate for locally advanced rectal cancer.[1–6]

Several studies have suggested that in selected patients with low rectal tumors, high-dose preoperative RT might permit the resection of the primary tumor with a high rate of preservation of sphincter function.[7–11] Such treatment results could have survival rates similar to those observed with more radical surgery without increasing the risk of pelvic or perineal recurrences.

However, except for a single European trial, definitive improvement in overall survival has not generally been demonstrated with preoperative RT alone.[3,12]

The prognosis of rectal cancer is generally related to the degree of penetration of the tumor through the bowel wall and the presence or absence of nodal involvement.[13–16] However, diagnostic accuracy of tumor penetration and nodal status is not sufficient.[17]

Many other prognostic markers have been evaluated retrospectively in determining the prognosis of patients with rectal cancer, although most, including allelic loss of chromosome 18q or thymidylate synthase expression, have not been prospectively validated.[18–20]

In those cases of rectal cancer in which preoperative RT was administered, nodal involvement and penetration of the tumor seemed to be significant for prognosis as well.[21–25] Besides nodal involvement and penetration status, no definitive prognostic markers have been reported in the preoperative radiation setting for this malignancy.

Prognostic information available before surgery is useful to select the candidates for a more aggressive surgical approach, such as extended lymphadenectomy, as well as intensive postoperative adjuvant therapy.[26–30] Also, the identification before the start of the entire treatment course of subsets of patients who are at low or high risk for recurrence can help to optimize treatment. For high-risk subsets, a more aggressive preoperative approach,

Address of correspondence: Keiichi Nakagawa, M.D., Ph.D., Department of Radiology, University of Tokyo Hospital, 7-3-1, Hongo, Bunkyo-ku, Tokyo 113-8655, Japan. E-mail: nakagawa-rad@umin.ac.jp

DOI: 10.1007/s10350-008-9243-2 • Volume 0: 1–6 (2008) • ©The ASCRS. 2008

such as combined modality preoperative treatment should be considered. Few predictors have been reported for this use.

Several studies have now been reported claiming the potential of fluorodeoxyglucose–positron emission tomography (FDG-PET) in predicting treatment outcome after preoperative RT for malignant neoplasms, including rectal cancer.[31,32] However, no consensus has been established on the usefulness of FDG-PET in predicting survival outcomes.

This study was designed to clarify the role of FDG-PET as a prognostic tool for patients with rectal cancer treated with preoperative RT.

PATIENTS AND METHODS

Study Design

From July 1995 to March 2002, the authors prospectively enrolled 59 patients with primary rectal cancer deemed eligible for preoperative RT, on the basis of a clinically bulky or tethered tumor or on imaging-based evidence of T3–4 or N1 disease by use of transrectal ultrasound. The distance from the anal edge of the tumor to the anal verge was <3 cm in 11 cases, 3 to 5 cm in 42 cases, and >5 cm in 6 cases. All patients received 50 Gy to the pelvis and were subjected to two series of FDG-PET: one before preoperative RT, and the other two to three weeks after the treatment (days after radiotherapy ranged from 11–50; mean, 17; median 16). Surgery was performed 20 to 77 (mean, 43.3; median, 41) days after the completion of preoperative RT and 3 to 63 (mean, 26.2; median, 25) days after the second FDG-PET study.

The study was a prospective trial and had institutional review board approval. Informed consent was obtained from all patients.

Treatments

For RT, a 6-MV x-ray accelerator delivered 50 Gy in 25 fractions, 5 fractions per week during five weeks. Two AP/PA opposed fields were used as a Japanese conventional radiation technique for pelvic tumors. The clinical target volume included the entire pelvic cavity, anal canal, primary tumor, mesorectal and presacral lymph nodes, nodes along the internal iliac artery, lumbar nodes up to the level of the lower border of the fifth lumbar vertebra, and nodes at the obturator foramen. No chemotherapy was added to the RT in a preoperative setting. All surgeries were performed by colorectal specialists. Abdominoperineal resection with permanent colostomy was performed mainly for low rectal cancers located <5 cm from the anal verge, and for other rectal cancers mainly intersphincteric resection with coloanal anastomosis, according to surgeons' judgment. When residual tumor cells were found in the surgical resection margin, postoperative adjuvant 5-fluorouracil–based chemotherapy was performed.

Positron Emission Tomography, Standardized Uptake Values

All patients received two series of FDG-PET: one before preoperative RT, and the other two to three weeks after the treatment (days after RT ranged from 11–50; mean days after RT, 17±7.6).[33] 18-fluorodeoxyglucose (18F) was synthesized using the Cypris Model 370 Cyclotron® (Sumitomo Heavy Industries, Shinagawa-ku, Tokyo, Japan), and FDG with an automated FDG synthesizer based on the method reported by Harms and Starling[11] radiochemical purity was >95 percent. The physical characteristics of this machine have been described in detail in a previous study.[31] Patients fasted for at least 4–1/2 hours before PET scanning so that serum glucose levels were between 80 and 110 mg/ml. All studies were performed using a Headtome IV dedicated PET scanner® (Shimadzu Corporation, Kyoto-city, Kyoto, Japan) with seven imaging planes at 13-mm intervals, each 10-mm thick. The inplane resolution was 4.5-mm full width at half maximum (FWHM). The axial resolution was 9.5-mm FWHM and the sensitivities were 14 and 24 kcps/(micro Ci/ml), respectively, for direct and cross planes. Each transmission scan was performed for eight minutes. For injections, 333 to 444 MBq of FDG were introduced via the cubital vein. A series of static acquisitions for 6 minutes each were initiated 60 minutes after the injection, and the mean time for the main tumor lesion was fixed at a constant setting of 63 minutes.

PET Data Analysis

Cross-sectional sinogram data were corrected for dead time, decay, random coincidences, and attenuation. Image reconstruction was performed by using a filtered back-projection algorithm with a Hanning filter using a cutoff frequency of 0.3 and a 128×128 matrix. Several regions of interest (ROIs) were drawn manually on the hot spots of tumors. To minimize the partial volume effect associated with decreasing tumor sizes resulting from radiotherapy, the ROIs were set to have a number of pixels between 40 and 99. FDG accumulation was measured by using standardized uptake values (SUV) obtained by the following equation:

$$\text{SUV} = (\text{decay corrected PET value})/[(\text{injected dose})/(\text{body weight})].$$ [33,34]

We defined SUVs in FDG-PET before preoperative RT as SUV_1 and two to three weeks after the treatment as SUV_2.

Pathologic Analysis

Analysis of the surgical specimen included a determination of the following parameters: 1) histologic type of the tumor; 2) degree of extension of the tumor through the rectal wall; 3) nodal involvement; and 4) status of proximal and distal margins. Pathologic response criteria were

Table 1. Univariate analysis

Factor	N	Relative risk	95% confidence interval	P value
Residual tumor				
+	8	1		
–	51	0.147	0.056–0.384	<0.0001
Differentiation				
Well	41	1		0.0011
Moderate	11	3.923	1.229–12.518	0.0210
Mucinous	4	6.14	1.57–24.012	0.0091
Poorly	2	23.093	4.09–130.371	0.0004
Unknown	1			
Recurrence				
+	31	1		
–	28	0.113	0.026–0.494	0.0038
Post-SUV	59	1.306	1.073–1.591	0.0079
SUV ratio				
>100%	4	1		
<100%	55	0.239	0.067–0.854	0.0276
LN				
+	30	1		
–	29	0.341	0.121–0.958	0.0411
Astler-Coller				
B1	10	0.21	0.027–1.63	0.1354
B2	18	0.315	0.088–1.132	0.0767
C1	4	1.123	0.247–5.097	0.8808
C2	26	1		0.1643
SUV ratio	59	1.014	0.994–1.033	0.1648
Pre-SUV	59	1.088	0.962–1.232	0.1788
Pathologic effect				
Grade 0	2	0.235	0.014–4.059	0.3193
Grade 1	44	0.102	0.012–0.868	0.0366
Grade 2	12	0.121	0.012–1.182	0.0693
Grade 3	1	1		0.1877
Sex				
Male	37	1		
Female	22	0.603	0.215–1.692	0.3363
Age (yr)	59	0.986	0.941–1.032	0.5392

SUV=standardized uptake values, LN=lymph node metastases.

defined as proposed by the Japanese Society for Esophageal Disease: Grade 0, no treatment effect; Grade 1, more than one-third viable tumor cells; Grade 2, less than one-third viable tumor cells; and Grade 3, no viable tumor cells.[35]

Statistical Analysis

Statistical analyses were performed by using StatView Dataset File version 5.0 J for Windows computers. Survival periods were calculated from the start of irradiation. The survival functions were estimated with the Kaplan-Meier method estimator, and log-rank tests were used to compare the survival distributions. Both univariate and multivariate analyses for survival were performed.

RESULTS

Pathologic effect and SUV ratio (SUV_2/SUV_1) were related statistically ($P=0.047$). Pathologic effect, however, showed no significant correlation with recurrence and survival. Histologic tumor type and SUV ratio were correlated and the ratio was >100 percent when the tumor type was poorly differentiated adenocarcinoma. Although recurrence rate tended to be higher with an elevated value of SUV_2, there was no significant association between them.

SUV ratio showed a tendency to be related with recurrence, and recurrence rate was of marginally higher significance when SUV ratio was >100 percent. Survival period was significantly short when SUV ratio was >100 percent ($P=0.0121$) and/or when SUV_2 was >5 ($P=0.0378$).

In univariate analysis, residual tumor, pathologic differentiation, recurrence, SUV_2 value, and lymph node metastasis were significant prognostic factors (Table 1). In multivariate analysis, no residual tumor and SUV_2 were significant prognostic factors for survival (Table 2). The survival curves comparing patients with *vs.* without residual tumor are shown in Fig. 1. Notably, when SUV_2 value was >5, overall survival was significantly poorer (Fig. 2). The median survival time and five-year overall survival rate comparing <5 *vs.* >5 SUV_2 value was 95.4 *vs.* 41.9 months and 70.4 *vs.* 43.6 percent, respectively ($P=0.042$).

DISCUSSION

SUV before RT and Prognosis

In this study, recurrence or poor prognosis was not related to high SUV before RT, which is in agreement with previously published reports. For head and neck cancers, Greven *et al.*[36] claimed that SUV before RT did not have any correlation with local control when examined for the entire group, primary site, or T stage (n=45). Others, however, have reported studies that differed from our results. Both Allal *et al.*[37] and Rege *et al.*[38] concluded that FDG uptake followed by RT, as measured by the SUV, had potential value in predicting local control and survival in head and neck carcinomas (n=63 and n=12, respectively).

SUV after RT and Prognosis

Recurrence or poor prognosis was related to high SUV after RT in our study. This result also concurs with earlier

Table 2. Multivariate analysis

Factor	Relative risk	95% confidence interval	P value
Residual tumor	0.302	0.094–0.973	0.0449
Differentiation			
Well			0.1552
Moderate	2.774	0.734–10.482	0.1326
Mucinous	2.875	0.574–14.406	0.1990
Poorly	10.486	0.988–111.283	0.0511
Recurrence	0.155	0.019–1.297	0.0854
Post-SUV	1.502	1.128–2	0.0054
SUV ratio <100%	0.675	0.107–4.268	0.6759
LN	0.362	0.080–1.637	0.1867

SUV=standardized uptake values; LN=lymph node metastases.

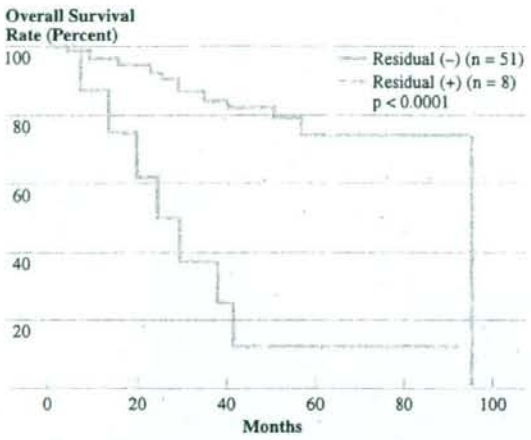

FIGURE 1. Overall survival curves comparing patients with *vs.* without residual tumor.

reports.[39,40] Higher SUV after preoperative RT predicts poor prognosis. Kunkel *et al.*[39] concluded that postirradiation FDG-uptake significantly predicted survival ($P=0.046$) and local tumor control ($P=0.0017$) in advanced oral squamous-cell carcinoma (n=35). Brun *et al.*[40] concluded that when a high initial tumor SUV was found, the reduction of SUV in the second PET examination might predict local tumor response in head and neck cancer (n=17). Swisher *et al.*[41] concluded that FDG-PET was predictive of survival in patients with esophageal carcinoma who had received preoperative chemoradiation ($P=0.01$; n=83). In our previous report,[32] only SUV_2 correlated with recurrence, although no significant correlation was observed in this study. It might be explained by the increased number of the patients involved to the study.

SUV before or after RT and Histologic Effects

SUV before or after RT was marginally correlated with histological effects. This finding is in agreement with previous reports. Kunkel *et al.*[42] reported a significant correlation ($P=0.045$) between post-RT FDG-uptake and histologic tumor regression was observed for mouth carcinoma (n=30). In their report, SUV>2.75 as a practical clinical threshold value for the identification of residual tumor resulted in a specificity of 88 percent, sensitivity of 68 percent, a positive predictive value of 94 percent, and a negative predictive value of 50 percent (in their report]).[41,42] In our actual follow-up data, a significant correlation could not be confirmed between post-RT SUV and patients' survivals. Brücher *et al.*[43] claimed an association for histology and survival in esophageal squamous-cell carcinoma (n=24). In responders, FDG uptake decreased by 72±11 percent; in nonresponders, it decreased by only 42±22 percent. Nonresponders to PET scanning (n=11) had a significantly poorer survival after resection than responders. Flamen *et al.*[44] also reported a correlation with histology and survival in locally advanced esophageal cancer (n=36). Response to chemoradiation as assessed by serial FDG-PET was strongly correlated with pathologic response ($P=0.002$) and survival ($P=0.087$).[44] In our study, SUV value after preoperative RT (SUV2) was significant in overall survival. In addition, the SUV ratio (SUV2/SUV1) showed an association with histopathologic effects and recurrence. These values are only available after the completion of preoperative radiation. In this respect, they may influence the surgical approach and postoperative adjuvant therapy. For example, if SUV1 was a prognostic marker, decisions could be made regarding preoperative treatment. SUV1 can control the entire treatment strategy, whereas SUV2 defines the surgical procedure and postoperative adjuvant therapy.

FDG-PET for Prediction of Survival in Rectal Cancer

The important implication of this study is that FDG-PET may be useful in assessing cytotoxic or ablative therapy. de Geus-Oei *et al.*[45] reported that a significant benefit ($P=0.017$) was observed in patients with low FDG uptake (SUV<4.26) with metastases of rectal cancer (of 152 patients, 67 were treated with resection of metastases and 85 with chemotherapy). A recent study from the Memorial Sloan-Kettering Cancer Center reported on monitoring the response to therapy with FDG-PET and the biologic basis of the change in FDG uptake of tumors in patients treated with neoadjuvant chemotherapy for hepatic colorectal metastases (13/42 evaluated patients underwent preoperative chemotherapy).[46] Fernandez *et al.*[47] concluded that post-resection screening by FDG-PET was associated with excellent five-year overall survival for patients undergoing resection of hepatic metastases from colorectal cancer (19 studies; 6,070 patients). Guillem *et al.*[48] from Memorial

FIGURE 2. Overall survival according to standardized uptake values-2 (SUV_2).

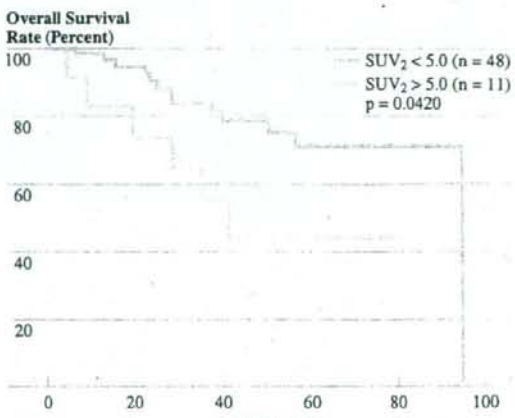

Sloan-Kettering Cancer Center suggested that FDG-PET might be useful in assessing the response of primary rectal cancer to chemoradiotherapy (n=15).

Denecke *et al.*[49] compared CT, MRI, and FDG-PET in the prediction of outcome of neoadjuvant radiochemotherapy in 23 patients with locally advanced primary T3/4 rectal cancer. The mean SUV reduction in responders (60±14 percent) was significantly higher than in nonresponders (37±31 percent; $P=0.03$). The sensitivity and specificity of FDG-PET in identifying response was 100 percent (CT 54 percent, MRI 71 percent) and 60 percent (CT 80 percent, MRT 67 percent). Positive and negative predictive values were 77 percent (CT 78 percent, MRI 83 percent) and 100 percent (CT 57 percent, MRI 50 percent) (PET $P=0.002$, CT $P=0.197$, MRI $P=0.5$). Additionally, Kalff *et al.*[50] evaluated the prognostic information obtained from the degree of change in tumor FDG-PET uptake induced by chemoradiation before radical curative surgery in 34 patients with T3/T4 rectal cancer. PET response was highly significantly associated with overall survival duration ($P<0.0001$) and time to progression ($P<0.0001$). Complete pathologic response was the only other statistically significant prognostic factor ($P<0.03$). The percentage of maximum SUV change after chemoradiation was not predictive of survival in partial metabolic response patients. Guillem *et al.*[31] tried to determine the prognostic significance of FDG-PET assessment of rectal cancer response to preoperative chemoradiation. The mean percentage decrease in SUV_{max} (ΔSUV_{max}) was 69 percent for patients free from recurrence and 37 percent for patients with recurrence ($P=0.004$). $\Delta SUV_{max} \geq 62.5$ was the best predictors of no-evidence-of-disease status and freedom from recurrence. Patients with $\Delta SUV_{max} \geq 62.5$ had significantly improved disease-specific and recurrence-free survival ($P=0.08$ and $P=0.03$, respectively).

The continued accumulation of clinical data on SUV for preoperative RT will contribute to establishing its usefulness. Studies in other malignancies, such as maxillary sinus carcinoma, are under consideration, for which preoperative RT is frequently performed.

CONCLUSION

A significant survival benefit was observed in patients with low FDG uptake (SUV<5) after preoperative radiotherapy in primary tumors of rectal cancer.

REFERENCES

1. Gerard A, Buyse M, Nordlinger B, *et al.* Preoperative radiotherapy as adjuvant treatment in rectal cancer: final results of randomized study (EORTC). Ann Surg 1988;208:606–14.
2. Anonymous. Preoperative short-term radiotherapy in operable rectal carcinoma: a prospective randomized trial. Stockholm Rectal Cancer Study Group. Cancer 1990;66:49–55.
3. Anonymous. Improved survival with preoperative radiotherapy in resectable rectal cancer. Swedish Rectal Cancer Trial. N Engl J Med 1997;336:980–7.
4. Colorectal Cancer Collaborative Group. Adjuvant radiotherapy for rectal cancer: a systematic overview of 8,507 patients from 22 randomised trials. Lancet 2001;358:1291–304.
5. Mendenhall WM, Millon RR, Bland KI, Pfaff WW, Copeland EM. Preoperative radiotherapy for clinically resectable adenocarcinoma of the rectum. Ann Surg 1985; 202:215–22.
6. Mohiuddin M, Marks G. Patterns of recurrence following high-dose preoperative radiation and sphincter-preserving surgery for cancer of the rectum. Dis Colon Rectum 1993; 36:117–26.
7. Mohiuddin M, Marks G. High dose preoperative irradiation for cancer of the rectum, 1976–1988. Int J Radiat Oncol Biol Phys 1991;20:37–43.
8. Ng AK, Recht A, Busse PM. Sphincter preservation therapy for distal rectal carcinoma: a review. Cancer 1997;79:671–83.
9. Mohiuddin M, Marks G, Bannon J. High-dose preoperative radiation and full thickness local excision: a new option for selected T3 distal rectal cancers. Int J Radiat Oncol Biol Phys 1994;30:845–9.
10. Willett CG. Organ preservation in anal and rectal cancers. Curr Opin Oncol 1996;8:329–33.
11. Harms BA, Starling JR. Current status of sphincter preservation in rectal cancer. Oncology (Williston Park) 1990;4:53–60.
12. Martling A, Holm T, Johansson H, Rutqvist LE, Cedermark B; Stockholm Colorectal Cancer Study Group. The Stockholm II trial on preoperative radiotherapy in rectal carcinoma: long-term follow-up of a population-based study. Cancer 2001;92:896–902.
13. Herrera L, Brown MT. Prognostic profile in rectal cancer. Dis Colon Rectum 1994;37:S1–5.
14. Tang R, Wang JY, Chen JS, *et al.* Survival impact of lymph node metastasis in TNM stage III carcinoma of the colon and rectum. J Am Coll Surg 1995;180:705–12.
15. Hojo K, Koyama Y, Moriya Y. Lymphatic spread and its prognostic value in patients with rectal cancer. Am J Surg 1982;144:350–4.
16. McLeod HL, Murray GI. Tumour markers of prognosis in colorectal cancer. Br J Cancer 1999;79:191–203.
17. Dershaw DD, Enker WE, Cohen AM, Sigurdson ER. Transrectal ultrasonography of rectal carcinoma. Cancer 1990;66:2336–40.
18. Wang WS, Lin JK, Chiou TJ, *et al.* Preoperative carcinoembryonic antigen level as an independent prognostic factor in colorectal cancer: Taiwan experience. Jpn J Clin Oncol 2000;30:12–6.
19. Jen J, Kim H, Piantadosi S, *et al.* Allelic loss of chromosome 18q and prognosis in colorectal cancer. N Engl J Med 1994;331:213–21.
20. Lanza G, Matteuzzi M, Gafa R, *et al.* Chromosome 18q allelic loss and prognosis in stage II and III colon cancer. Int J Cancer 1998;79:390–5.
21. Rinkus KM, Russell GB, Levine EA. Prognostic significance of nodal disease following preoperative radiation for rectal adenocarcinoma. Ann Surg 2002;68:482–7.

22. Myerson RJ, Michalski JM, King ML, *et al.* Adjuvant radiation therapy for rectal carcinoma: predictors of outcome. Int J Radiat Oncol Biol Phys 1995;32:547–8.
23. Onaitis MW, Noone RB, Hartwig M, *et al.* Neoadjuvant chemoradiation for rectal cancer: analysis of clinical outcomes from a 13-year institutional experience. Ann Surg 2001;233:778–85.
24. Theodoropoulos G, Wise WE, Padmanabhan A, *et al.* T-level downstaging and complete pathologic response after preoperative chemoradiation for advanced rectal cancer result in decreased recurrence and improved disease-free survival. Dis Colon Rectum 2002;45:895–903.
25. Mohiuddin M, Hayne M, Regine WF, *et al.* Prognostic significance of postchemoradiation stage following preoperative chemotherapy and radiation for advanced/recurrent rectal cancers. Int J Radiat Oncol Biol Phys 2000;48:1075–80.
26. Moriya Y, Sugihara K, Akasu T, Fujita S. Importance of extended lymphadenectomy with lateral node dissection for advanced lower rectal cancer. World J Surg 1997;21:728–32.
27. Moriya Y, Hojo K, Sawada T, Koyama Y. Significance of lateral node dissection for advanced rectal carcinoma at or below the peritoneal reflection. Dis Colon Rectum 1989;32:307–15.
28. Minsky BD. Adjuvant therapy for rectal cancer: the transatlantic view. Colorectal Dis 2003;5:416–22.
29. Rodel C, Sauer R. Perioperative radiotherapy and concurrent radiochemotherapy in rectal cancer. Semin Surg Oncol 2001;20:3–12.
30. Wils J, O'Dwyer P, Labianca R. Adjuvant treatment of colorectal cancer at the turn of the century: European and US perspectives. Ann Oncol 2001;12:13–22.
31. Guillem JG, Moore HG, Akhurst T, *et al.* Sequential preoperative fluorodeoxyglucose-positron emission tomography assessment of response to preoperative chemoradiation: a means for determining long term outcomes of rectal cancer. J Am Coll Surg 2004;199:1–7.
32. Oku S, Nakagawa K, Momose T, *et al.* FDG-PET after radiotherapy is a good prognosis indicator of rectal cancer. Ann Nucl Med 2002;16:409–16.
33. Kanno I, Iida H, Miura S, *et al.* Design concepts and preliminary performances of stationary-sampling whole-body high-resolution positron emission tomography: HEADTOME IV [in Japanese]. Kaku Igaku 1989;26:477–85.
34. Zasadny KR, Wahl RL. Standardized uptake values of normal tissues at PET with 2-[fluorine-18]-fluoro-2-deoxy-D-glucose: variations with body weight and a method for correction. Radiology 1993;189:847–50.
35. The Japanese Society for Esophageal Disease. Histopathologic criteria for the effects of radiation or anticancer chemotherapy. In: Isono K, ed. Guidelines for clinical and pathologic studies on carcinoma of the esophagus. 9th ed. Tokyo: Kanehara Shuppan, 1999:55.
36. Greven KM, Williams DW III, McGuirt WF Sr, *et al.* Serial positron emission tomography scans following radiation therapy of patients with head and neck cancer. Head Neck 2001;23:942–6.
37. Allal AS, Dulguerov P, Allaoua M, *et al.* Standardized uptake value of 2-[(18)F] fluoro-2-deoxy-D-glucose in predicting outcome in head and neck carcinomas treated by radiotherapy with or without chemotherapy. J Clin Oncol 2002;20:1398–404.
38. Rege S, Safa AA, Chaiken L, Hoh C, Juillard G, Withers HR. Positron emission tomography: an independent indicator of radiocurability in head and neck carcinomas. Am J Clin Oncol 2000;23:164–9.
39. Kunkel M, Forster GJ, Reichert TE, *et al.* Radiation response non-invasively imaged by [18F]FDG-PET predicts local tumor control and survival in advanced oral squamous cell carcinoma. Oral Oncol 2003;39:170–7.
40. Brun E, Ohlsson T, Erlandsson K, *et al.* Early prediction of treatment outcome in head and neck cancer with 2–18FDG PET. Acta Oncol 1997;36:741–7.
41. Swisher SG, Erasmus J, Maish M, *et al.* 2-Fluoro-2-deoxy-D-glucose positron emission tomography imaging is predictive of pathologic response and survival after preoperative chemoradiation in patients with esophageal carcinoma. Cancer 2004;101:1776–85.
42. Kunkel M, Grotz KA, Forster GJ, *et al.* Therapy monitoring with 2-(18F)-FDG positron emission tomography after neoadjuvant radiation treatment of mouth carcinoma [in German]. Srahlenther Onkol 2001;177:145–52.
43. Brücher BL, Weber W, Bauer M, *et al.* Neoadjuvant therapy of esophageal squamous cell carcinoma: response evaluation by positron emission tomography. Ann Surg 2001;233:300–9.
44. Flamen P, Van Cutsem E, Lerut A, *et al.* Positron emission tomography for assessment of the response to induction radiochemotherapy in locally advanced oesophageal cancer. Ann Oncol 2002;13:361–8.
45. de Geus-Oei LF, Wiering B, Krabbe PF, Ruers TJ, Punt CJ, Oyen WJ. FDG-PET for prediction of survival of patients with metastatic colorectal carcinoma. Ann Oncol 2006;17:1650–5.
46. Akhurst T, Kates TJ, Mazumdar M, *et al.* Recent chemotherapy reduces the sensitivity of [18F]fluorodeoxyglucose positron emission tomography in the detection of colorectal metastases. J Clin Oncol 2005;23:8713–6.
47. Fernandez FG, Drebin JA, Linehan DC, Dehdashti F, Siegel BA, Strasberg M. Five-year survival after resection of hepatic metastases from colorectal cancer in patients screened by positron emission tomography with F-18 fluorodeoxyglucose (FDG-PET). Ann Surg 2004;240:438–5.
48. Guillem JG, Puig-La Calle J Jr, Akhurst T, *et al.* Prospective assessment of primary rectal cancer response to preoperative radiation and chemotherapy using 18-fluorodeoxyglucose positron emission tomography. Dis Colon Rectum 2000;43:18–24.
49. Denecke T, Rau B, Hoffmann KT, *et al.* Comparison of CT, MRI and FDG-PET in response prediction of patients with locally advanced rectal cancer after multimodal preoperative therapy: is there a benefit in using functional imaging? Eur Radiol 2005;15:1658–66.
50. Kalff V, Duong C, Drummond EG, Matthews JP, Hicks RJ. Findings on 18F-FDG PET scans after neoadjuvant chemoradiation provides prognostic stratification in patients with locally advanced rectal carcinoma subsequently treated by radical surgery. J Nucl Med 2006;47:14–22.

Jpn J Clin Oncol 2008;38(6)438–444
doi:10.1093/jjco/hyn038

Three-dimensional Conformal Radiotherapy for Hepatocellular Carcinoma with Inferior Vena Cava Invasion

Hiroshi Igaki[1], Keiichi Nakagawa[1], Kenshiro Shiraishi[1], Shuichiro Shiina[2], Norihiro Kokudo[3], Atsuro Terahara[1], Hideomi Yamashita[1], Nakashi Sasano[1], Masao Omata[2] and Kuni Ohtomo[1]

[1]Departments of Radiology, [2]Gastroenterology and [3]Hepato-Biliary-Pancreatic Surgery, The University of Tokyo Hospital, Tokyo, Japan

Received February 25, 2008; accepted April 24, 2008; published online May 21, 2008

Background: Hepatocellular carcinoma with inferior vena cava invasion is a rare but fatal condition of disease progression. The aim of this study was to analyze the results of treatment for hepatocellular carcinoma with inferior vena cava invasion by three-dimensional conformal radiation therapy.

Methods: From 1990 to 2006, 18 histopathologically confirmed hepatocellular carcinoma patients with inferior vena cava invasion who were unsuitable for surgery were treated by three-dimensional conformal radiation therapy at our hospital with two to four static or dynamic conformal arc fields.

Results: A median total tumor dose of 50 Gy (range 30–60 Gy) was delivered. The progression-free rate was 91.6% among the patients in whom follow-up computed tomography was obtained. Actuarial survival at 1 year was 33.3%, and the median survival period was 5.6 months.

Conclusions: Three-dimensional conformal radiation therapy might offer a chance of long survival for a part of the hepatocellular carcinoma patients with inferior vena cava invasion, since a third of such patients survived more than a year. Additional treatments should be considered to prevent distant metastases and hepatic functional deterioration after three-dimensional conformal radiation therapy.

Key words: hepatocellular carcinoma – inferior vena cava – three-dimensional conformal radiation therapy – hepatic functional reserve – liver cirrhosis

INTRODUCTION

Hepatocellular carcinoma (HCC) is the eighth major cause of cancer death in the United States and the third in Japan (1,2). Local ablative therapies such as hepatectomy, radiofrequency ablation (RFA) and percutaneous ethanol injection (PEI) should be administered, if possible, to patients with limited extension of HCC. But when the tumor invades the inferior vena cava (IVC), these treatments are indicated only for very few patients. In some reports, a part of these patients can survive long by hepatic resection combined with IVC resection (3–5). But such aggressive surgeries are not suitable for most patients, and other treatment modalities are also restricted not only by poor hepatic function, but also frequently by extensive disease progression. Transcatheter arterial chemoembolization (TACE) is often tried in HCC patients with IVC invasion for whom ablative treatment is unsuitable. However, TACE rarely achieves local tumor control to prolong survival periods sufficiently in such a critical condition, although the efficacy of this treatment has been proven in meta-analyses (6,7).

A few decades ago, liver was assumed to be a highly radiosensitive organ that was unsuitable for high-dose radiotherapy. But recent progress in radiation oncology has enabled us to concentrate high-dose radiation on liver tumors while preserving hepatic function after treatment (8–15). In addition, some institutions apply stereotactic radiotherapy to solitary small liver tumors. Consequently, radiotherapy has come to play an important role in multidisciplinary treatment of HCC.

At our institution, three-dimensional conformal radiation therapy (3D-CRT) has been the primary treatment strategy for HCC with portal vein invasion, and has achieved good clinical results (9). As with the treatment of HCC patients

For reprints and all correspondence: Hiroshi Igaki, Department of Radiology, The University of Tokyo Hospital, 7-3-1, Hongo, Bunkyo-ku, Tokyo 113-8655, Japan. E-mail: igaki-tky@umin.ac.jp

with portal vein invasion, radiotherapy is considered for HCC patients with IVC invasion at our institution if they are unsuitable for surgery. But there are few reports on radiotherapy for such patients (16), and the natural course of such conditions is not well known. In the present study, we retrospectively reviewed the medical records of HCC patients with IVC invasion and analyzed the efficacy of radiotherapy in these patients.

METHODS

From 1990 to 2006, 18 HCC patients with IVC invasion were treated by radiotherapy at our hospital. Their clinical courses and treatment results were retrospectively reviewed. HCC was diagnosed by using ultrasonography, computed tomography (CT), angiography and liver biopsy. In each patient, the diagnosis was confirmed histopathologically. IVC invasion was defined by a low-attenuation mass that protruded into the intraluminal space of IVC on enhanced CT and/or detection of pulsatile flow in IVC thrombi by Doppler ultrasonography. The patients' characteristics are shown in Table 1.

Patients with liver cirrhosis of Child–Pugh class C were not indicated for the treatment. CT-based radiotherapy treatment planning was made for all patients by the following treatment planning systems, RPS700U(3D) (Mitsubishi Electric Co., Tokyo, Japan) or Pinnacle[3] (Philips/ADAC, Milpitas, CA, USA). Clinical target volume was contoured on serial CT images with a 0.5–1-cm margin around the gross tumor volume, covering IVC-protruding tumor as well as the primary tumor invading to the IVC. Other co-existing intrahepatic tumors which had no continuity to the IVC-invading tumor were not included in the clinical target volume, and managed by other treatment modalities. Planning target volume was determined by a 0.5–2.0-cm margin around the clinical target volume. A dynamic conformal arc or two to four static ports were used for irradiation. In earlier periods, dynamic conformal arc therapy or multiport (mainly four ports) treatment plans were used, and we could not obtain dose-volume histograms in the treatment-planning machine. In recent years, treatment plans using two opposed fields have been preferred, because such treatment enables the maximization of the non-irradiated volume of the normal liver tissue. This treatment planning strategy is based on the fact that the normal liver tissue tolerance is lower in patients with viral hepatitis and liver cirrhosis than

Table 1. Patient characteristics

Case no.	Age and sex	Previous treatment				Etiology	Child–Pugh class	Pre-treatment AFP (ng/mL)[1]	Pre-treatment PIVKAII (mAu/mL)[2]
		Surgery	TACE	PEI	RFA				
1	48M	Information not available				HBV	A	38	1
2	67M	Information not available				HBV	B	60	8
3	63M	○		○		Unknown	A	9	N/A
4	67M			○		HCV	A	2385	125
5	80F	Information not available				HCV	A	3	1134
6	58M		○			Alcohol	B	9	26622
7	45M	○	○			HBV	B	136260	10784
8	71M		○		○	HCV	B	4	3242
9	74M		○			HCV	B	10	88
10	70M		○			HCV	B	13	7207
11	61M		○			HCV	B	21	3639
12	72M	○	○	○	○	HCV	A	6175	28
13	70M		○			HCV	B	126	39
14	76M		○			HCV	B	20	3572
15	71M	○	○			HCV	A	11	538
16	74M		○	○	○	HCV	A	38	681
17	69F		○		○	HCV	B	8	1119
18	81M	○	○	○	○	HCV	A	1	12008

Open circles indicate that the patient has received the specific treatment(s). M, male; F, female; TACE, transcatheter arterial chemoembolization; PEI, percutaneous ethanol injection; RFA, radiofrequency ablation; HBV, hepatitis B virus; HCV, hepatitis C virus; N/A, not available; PIVKAII, protein induced by Vitamin K absence-II.

[1]Normal range of serum concentration of AFP is <9 ng/mL.

[2]Normal range of serum concentration of PIVKAII is <40 mAu/mL.

in healthy patients (8). The general principle of treatment planning was to keep V_{30}, which was defined as the percent volume of the liver exceeding 30 Gy, lower than 30% of the whole liver volume minus tumor volume. We aimed for a total tumor dose of 50–60 Gy in conventional fractionation, but allowed smaller doses according to the dose-volume histogram of the normal liver at the physician's discretion. X-rays were delivered by linear accelerators ML15-MDX (Mitsubishi Electric Co., Tokyo, Japan) or CRS-6000 (Mitsubishi Electric Co., Tokyo, Japan). Written informed consent was obtained from the patients before treatment.

Follow-up and survival periods were calculated from the first day of radiation therapy. Actuarial survival rates were calculated by the Kaplan–Meier method. The statistical significance between groups was assessed with the log-rank test. Differences were considered statistically significant when $P < 0.05$.

RESULTS

All patients tolerated the treatment well. No severe complications were observed during the treatment period. The total tumor dose ranged from 30 to 60 Gy, with a median dose of 50 Gy (Table 2). All patients were followed until death except for the three patients who were alive at the time of analysis. Other treatment variables and results are summarized in Table 2.

Treatment response was defined as the tumor status at the last follow-up CT (Table 2). The response rate (complete response + partial response) and progression-free rate (complete response + partial response + stable disease) were 33.3% (95% confidential interval: 6.7–60.0%) and 91.6% (95% confidential interval: 75.9–100%), respectively, among the 12 patients for whom follow-up CTs were obtained. Only one patient developed local progression of the IVC-invading tumor within 6 months after 3D-CRT, and this was determined to be a progressive disease. This patient started systemic chemotherapy with 5-fluorouracil and interferon after diagnosis of a progressive disease, and was alive at the time of this analysis with no further progression of the tumor after introduction of this chemotherapy, 26.2 months after treatment. In the remaining 11 patients, no tumor regrowth was observed within the irradiated volume at the last follow-up.

At the time of the last follow-up, three patients were alive and the others were dead. Actuarial survival rate was 33.3% at 1 year, with a median survival period of 5.6 months (Fig. 1). The causes of death are shown in Table 2. The Child–Pugh class A group tended to survive longer than the class B group, but the difference did not reach statistical significance level (7.8 months versus 3.3 months, $P = 0.136$, Fig. 2 and Table 3). The survival period did not differ between responders (complete response + partial response) and non-responders (stable disease + progressive disease) (Fig. 3 and Table 3). Older patients (70 years or older) and

Table 2. Treatment-related variables and results

Case no.	Total dose (Gy)	Equivalent dose (Gy)[1]	Irradiation technique	Treatment response	Follow-up period (months)	Cause of death
1	48	52	Opposed two fields	N/A	5.6	Unknown
2	48	52	Dynamic conformal	N/A	3.0	Unknown
3	30	37.5	Dynamic conformal	N/A	7.2	Unknown
4	42	42	Dynamic conformal	N/A	1.3	Pulmonary metastasis
5	60	60	Dynamic conformal	CR	7.8	Non-tumoral Liver failure
6	50	50	Dynamic conformal	N/A	3.7	Rupture of esophageal varix
7	50	50	Four fields	SD	3.3	Tumor-related Liver failure
8	46	46	Four fields	SD	2.6	Non-tumoral Liver failure
9	50	50	Four fields	PR	7.2	Pulmonary metastasis
10	50	50	Dynamic conformal	PR	16.3	Non-tumoral Liver failure
11	40	40	Four fields	SD	1.8	Pulmonary metastasis
12	50	50	Dynamic conformal	CR	13.7	Tumor-related Liver failure
13	52	52	Four fields	N/A	1.6	Pulmonary embolization
14	46	46	Opposed two fields	SD	4.7	Tumor-related Liver failure
15	50	50	Four fields	SD	14.5	Brain metastasis
16	50	50	Non-coplanar	PD	26.2	(Alive)
17	40	40	Opposed two fields	SD	12.6	(Alive)
18	50	50	Opposed two fields	SD	10.2	(Alive)

CR, complete response; PR, partial response; SD, stable disease; PD, progressive disease.
[1]Equivalent dose in conventional fractionation of 2.0 Gy per fraction was calculated based on a linear quadratic model assuming $\alpha/\beta = 10$ (32).

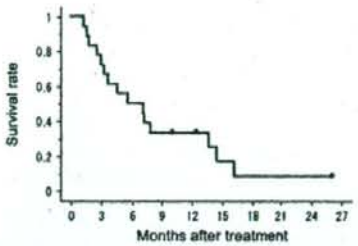

Figure 1. Overall survival of the whole group of 18 patients.

patients with hepatitis C virus tended to survive longer than the other patients, but the differences were also not statistically significant (Fig. 4). The median survival periods were 7.8 and 3.3 months for the groups 70 years or older and under 70 years, respectively ($P = 0.064$). The median survival periods of the patients with HCV carriers and other etiologies were 7.8 and 3.7 months, respectively ($P = 0.111$). A representative case is shown in Fig. 5.

Table 3. Univariate analysis of potential prognostic factors

Factor	*n*	Median survival (months)	*P* value
Etiology			
HCV	13	7.8	0.111
Others	5	3.7	
Treatment response			
Responders	4	7.8	0.894
Non-responders	8	4.6	
Age at treatment			
≥ 70	10	7.8	0.064
< 70	8	3.3	
Child–Pugh class			
A	8	7.8	0.136
B	10	3.3	
Pre-treatment AFP			
≤ 20 ng/mL	10	7.2	0.305
> 20 ng/mL	8	3.0	
Pre-treatment PIVKA II			
≤ 1000 mAu/mL	9	5.6	0.987
> 1000 mAu/mL	9	4.7	

DISCUSSION

HCC with IVC invasion is difficult to treat and associated with poor prognosis, because of its inherent nature of serious condition of the disease and the limited availability of treatment strategies. We have treated such patients by 3D-CRT, and here reviewed their treatment results retrospectively.

The literature offers no detailed data on the natural history of HCC with IVC invasion. But vascular invasion from HCC has been associated with miserable prognoses (16–18) and a limited life expectancy of 2–3 months, if untreated. However, Mizumoto et al. (19) reported good clinical results of proton beam therapy in patients with HCC invading to the IVC. All three of the patients they treated lived more than a year after this therapy.

The prognosis of patients with HCC is known to be dependent on the hepatic functional reserve (20,21). Our results are consistent with this knowledge, because the median survival of Child–Pugh class A patients was slightly longer than that of class B patients (Fig. 2). On the other hand, treatment response did not influence patients' survival periods (Fig. 3). But the treatment response after radiotherapy is predictive of survival in the curative treatment settings in many primary cancer sites (22–24). There are three possible explanations for this: (i) a relatively long period (typically several months) is required for tumor shrinkage after radiotherapy, considering the median survival periods of these patients; (ii) fatal deterioration of hepatic function can be seen, owing to the damage to normal liver tissue as a result of radiotherapy; (iii) it is sometimes difficult to distinguish the tumor thrombus from blood clots adhering to the IVC-invading tumor on follow-up CT images; and (iv) the group in this analysis was too small for statistical differences. Older age was a marginally significant prognostic factor in our results (Fig. 4). Age as a prognostic factor,

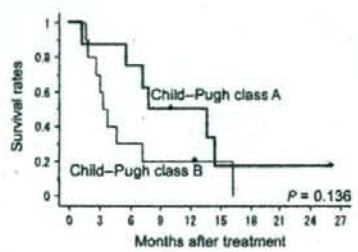

Figure 2. Overall survival by pre-treatment hepatic functional reserve.

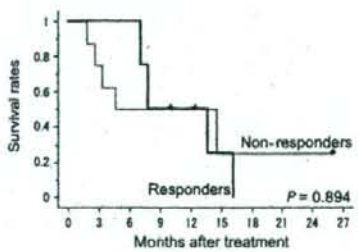

Figure 3. Overall survival by treatment response.

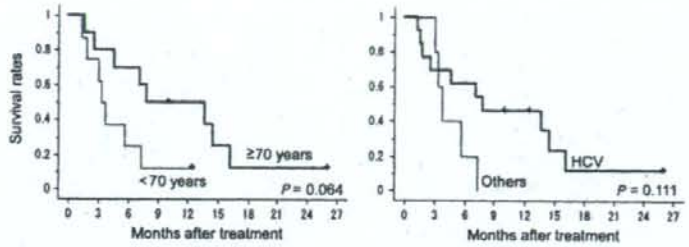

Figure 4. Overall survival by age (left panel) or etiology (right panel).

however, is controversial in the literature, because older age might sometimes be a favorable prognostic factor in some conditions but an unfavorable one in others (25–27).

In our experience, six patients died of liver failure. Of these six, three were assumed to be owing to the intrahepatic tumor growth from their clinical courses, and the other three were brought by undetermined causes. We could not differentiate the natural course of cirrhosis from treatment-related liver failure exactly. In this respect, we could not exclude the possibility of the treatment-related morbidities in Cases 5, 8 and 10 in Tables 1 and 2 with liver failures, although there had been no case with clinically apparent radiation-induced liver disease (RILD). In addition, there is no denying that the rupture of esophageal varix and the pulmonary embolization have occurred irrelevant to 3D-CRT or other treatments in Cases 6 and 13. But after 3D-CRT, 33.3% of our patients survived more than a year. In this respect, our 3D-CRT appeared to offer a chance to survive more than a year for a third of the patients with such critical conditions, although the median survival period was not satisfactory. The reason for such unsatisfactory results included the high incidence of deaths due to metastatic disease or liver failure despite the good progression-free rate of 91.6% for the irradiated IVC-invading tumor.

To minimize the probability of radiotherapy-related liver failure, treatment strategies have been improved (28,29). Despite these efforts, RILD can sometimes occur typically 2 weeks to 4 months after hepatic irradiation, and the threshold for RILD is reported to be 31 Gy of mean liver dose (29). Moreover, 50–76% of the patients who developed RILD died of this complication (30,31). Considering these situations, 3D-CRT has a potential benefit over the conventional two-dimensional radiotherapy in the viewpoint of normal liver protection. This point, however, has not been demonstrated in the previous literature to the best of our knowledge.

Some institutions adopt stereotactic body radiotherapy by multi-port irradiation technique. But the volume of low-dose-irradiated normal liver tissue is increased by the multi-port irradiation, especially when the clinical target volume is large. Radiation tolerance of the non-cancerous liver with chronic viral hepatitis or cirrhosis is known to be lower than that of healthy liver (29). We have a hypothesis that two opposed fields radiotherapy might be more protective than multiple-port radiotherapy for the cirrhotic liver. This is why we changed the 3D-CRT strategy from multiple-port irradiation to two opposed fields irradiation. We are now under investigation of the effect of treatment strategy on the survival or on the risk of RILD.

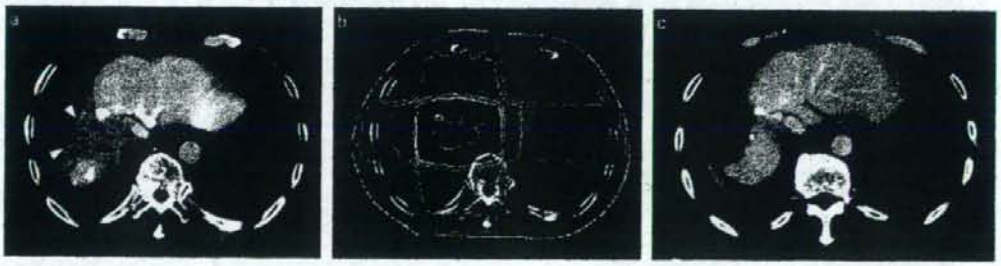

Figure 5. A representative case of a 72-year-old male with Child–Pugh class A hepatic function (case 12 in the Tables 1 and 2). (a) Before radiotherapy, the tumor located in S7 extended to IVC and the intraluminal space was narrow in the CT images. The tumor was indicated by the red arrowhead. (b) Dose distribution of the treatment plan. A total tumor dose of 50 Gy was delivered in 25 fractions by a dynamic conformal arc with four static fields. (c) Three months after radiotherapy. S7 tumor disappeared and no enhancement defect was observed within IVC, and the treatment response was judged as a complete response. The patient died of hepatic failure 13.7 months after irradiation. The irradiated tumor had no sign of regrowth at the time of death. (A colour version of this figure is available as supplementary data at http://www.jjco.oxfordjournals.org.)

Follow-up CT could not be obtained for six patients. This might be attributable in part to early deterioration in performance status, since all six died within 8 months after treatment. It is possible that disease control was not achieved in these patients and that the progression-free rate of 91.6% was thus overestimated. In this respect, additional treatments should be considered as many patients developed distant metastases or hepatic functional deterioration shortly after 3D-CRT.

CONCLUSIONS

A part of the HCC patients with IVC invasion might have benefited from 3D-CRT and a third of such patients had had a chance of surviving more than a year; otherwise they could not have survived long with this progressive fatal disease. However, further treatment should be considered to prevent distant metastasis and to protect post-treatment hepatic function, because the majority of the patients died from metastatic diseases or liver failure in spite of good local tumor control by 3D-CRT.

Funding

This work was supported by grants-in-aid for scientific research from the Ministry of Education, Science, and Culture of Japan (18790877 to H.I.).

Conflict of interest statement

None declared.

References

1. Surveillance Epidemiology and End Results NCI, US National Institute of Health [homepage on the Internet]. Summary of changes in cancer mortality, 1950–2004 and 5-year relative survival rates, 1950–2003 [cited 2008 February 26]. Available format: http://seer.cancer.gov/csr/1975_2004/results_single/sect_01_table.03.pdf.
2. Center for Cancer Control and Information Services, National Cancer Center, Japan [homepage on the Internet]. Graph database, Cancer information service for medical staff [cited 2008 February 26]. Available at: http://ganjoho.ncc.go.jp/pro/statistics/en/graph_db_index.html.
3. Arii S, Teramoto K, Kawamura T, Takamatsu S, Sato E, Nakamura N, et al. Significance of hepatic resection combined with inferior vena cava resection and its reconstruction with expanded polytetrafluoroethylene for treatment of liver tumors. *J Am Coll Surg* 2003;196:243–9.
4. Sarmiento JM, Bower TC, Cherry KJ, Farnell MB, Nagorney DM. Is combined partial hepatectomy with segmental resection of inferior vena cava justified for malignancy? *Arch Surg* 2003;138:624–30; discussion 630–1.
5. Hemming AW, Reed AI, Langham MR, Jr, Fujita S, Howard RJ. Combined resection of the liver and inferior vena cava for hepatic malignancy. *Ann Surg* 2004;239:712–9; discussion 719–21.
6. Cammà C, Schepis F, Orlando A, Albanese M, Shahied L, Trevisani F, et al. Transarterial chemoembolization for unresectable hepatocellular carcinoma: meta-analysis of randomized controlled trials. *Radiology* 2002;224:47–54.
7. Llovet JM, Bruix J. Systematic review of randomized trials for unresectable hepatocellular carcinoma: chemoembolization improves survival. *Hepatology* 2003;37:429–42.
8. Dawson LA, Ten Haken RK. Partial volume tolerance of the liver to radiation. *Semin Radiat Oncol* 2005;15:279–83.
9. Nakagawa K, Yamashita H, Shiraishi K, Nakamura N, Tago M, Igaki H, et al. Radiation therapy for portal venous invasion by hepatocellular carcinoma. *World J Gastroenterol* 2005;11:7237–41.
10. Huang CJ, Lian SL, Chen SC, Wu DK, Wei SY, Huang MY, et al. External beam radiation therapy for inoperable hepatocellular carcinoma with portal vein thrombosis. *Kaohsiung J Med Sci* 2001;17:610–4.
11. Tazawa J, Maeda M, Sakai Y, Yamane M, Ohbeyashi H, Kakinuma S, et al. Radiation therapy in combination with transcatheter arterial chemoembolization for hepatocellular carcinoma with extensive portal vein involvement. *J Gastroenterol Hepatol* 2001;16:660–5.
12. Ishikura S, Ogino T, Furuse J, Satake M, Baba S, Kawashima M, et al. Radiotherapy after transcatheter arterial chemoembolization for patients with hepatocellular carcinoma and portal vein tumor thrombus. *Am J Clin Oncol* 2002;25:189–93.
13. Yamada K, Izaki K, Sugimoto K, Mayahara H, Morita Y, Yoden E, et al. Prospective trial of combined transcatheter arterial chemoembolization and three-dimensional conformal radiotherapy for portal vein tumor thrombus in patients with unresectable hepatocellular carcinoma. *Int J Radiat Oncol Biol Phys* 2003;57:113–9.
14. Kim DY, Park W, Lim DH, Lee JH, Yoo BC, Paik SW, et al. Three-dimensional conformal radiotherapy for portal vein thrombosis of hepatocellular carcinoma. *Cancer* 2005;103:2419–26.
15. Lin CS, Jen YM, Chiu SY, Hwang JM, Chao HL, Lin HY, et al. Treatment of portal vein tumor thrombosis of hepatoma patients with either stereotactic radiotherapy or three-dimensional conformal radiotherapy. *Jpn J Clin Oncol* 2006;36:212–7.
16. Zeng ZC, Fan J, Tang ZY, Zhou J, Qin LX, Wang JH, et al. A comparison of treatment combinations with and without radiotherapy for hepatocellular carcinoma with portal vein and/or inferior vena cava tumor thrombus. *Int J Radiat Oncol Biol Phys* 2005;61:432–43.
17. Llovet JM, Bustamante J, Castells A, Vilana R, Ayuso Mdel C, Sala M, et al. Natural history of untreated nonsurgical hepatocellular carcinoma: rationale for the design and evaluation of therapeutic trials. *Hepatology* 1999;29:62–7.
18. The Cancer of the Liver Italian Program (CLIP) Investigators. A new prognostic system for hepatocellular carcinoma: a retrospective study of 435 patients. *Hepatology* 1998;28:751–5.
19. Mizumoto M, Tokuuye K, Sugahara S, Hata M, Fukumitsu N, Hashimoto T, et al. Proton beam therapy for hepatocellular carcinoma with inferior vena cava tumor thrombus: report of three cases. *Jpn J Clin Oncol* 2007;37:459–62.
20. Franco D, Capussotti L, Smadja C, Bouzari H, Meakins J, Kemeny F, et al. Resection of hepatocellular carcinomas: results in 72 European patients with cirrhosis. *Gastroenterology* 1990;98:733–8.
21. Okuda K. Natural history of hepatocellular carcinoma including fibrolamellar and hepato-cholangiocarcinoma variants. *J Gastroenterol Hepatol* 2002;17:401–5.
22. Chen CH, Chang TT, Cheng KS, Su WW, Yang SS, Lin HH, et al. Do young hepatocellular carcinoma patients have worse prognosis? The paradox of age as a prognostic factor in the survival of hepatocellular carcinoma patients. *Liver Int* 2006;26:766–73.
23. Liem MS, Poon RT, Lo CM, Tso WK, Fan ST. Outcome of transarterial chemoembolization in patients with inoperable hepatocellular carcinoma eligible for radiofrequency ablation. *World J Gastroenterol* 2005;11:4465–71.
24. Wu DH, Liu L, Chen LH. Therapeutic effects and prognostic factors in three-dimensional conformal radiotherapy combined with transcatheter arterial chemoembolization for hepatocellular carcinoma. *World J Gastroenterol* 2004;10:2184–9.
25. Kayama T, Kumabe T, Tominaga T, Yoshimoto T. Prognostic value of complete response after the initial treatment for malignant astrocytoma. *Neurol Res* 1996;18:321–4.
26. Willers H, Wurschmidt F, Bunemann H, Heilmann HP. High-dose radiation therapy alone for inoperable non-small cell lung cancer—experience with prolonged overall treatment times. *Acta Oncol* 1998;37:101–5.
27. Kostakoglu L, Goldsmith SJ. PET in the assessment of therapy response in patients with carcinoma of the head and neck and of the esophagus. *J Nucl Med* 2004;45:56–68.
28. Lawrence TS, Robertson JM, Anscher MS, Jirtle RL, Ensminger WD, Fajardo LF. Hepatic toxicity resulting from cancer treatment. *Int J Radiat Oncol Biol Phys* 1995;31:1237–48.

29. Dawson LA, Normolle D, Balter JM, McGinn CJ, Lawrence TS, Ten Haken RK. Analysis of radiation-induced liver disease using the Lyman NTCP model. *Int J Radiat Oncol Biol Phys* 2002;53:810–21.
30. Cheng JC, Wu JK, Huang CM, Liu HS, Huang DY, Cheng SH, et al. Radiation-induced liver disease after three-dimensional conformal radiotherapy for patients with hepatocellular carcinoma: dosimetric analysis and implication. *Int J Radiat Oncol Biol Phys* 2002;54: 156–62.
31. Xu ZY, Liang SX, Zhu J, Zhu XD, Zhao JD, Lu HJ, et al. Prediction of radiation-induced liver disease by Lyman normal-tissue complication probability model in three-dimensional conformal radiation therapy for primary liver carcinoma. *Int J Radiat Oncol Biol Phys* 2006;65: 189–95.
32. Fowler JF. The linear–quadratic formula and progress in fractionated radiotherapy. *Br J Radiol* 1989;62:679–94.

Acta Oncologica, 2009; 48: 314–318

informa
healthcare

LETTERS TO THE EDITOR

Contrast media-assisted visualization of brain metastases by kilovoltage cone-beam CT

HIROSHI IGAKI[1], KEIICHI NAKAGAWA[1], HIDEOMI YAMASHITA[1], ATSURO TERAHARA[1], AKIHIRO HAGA[1], KENSHIRO SHIRAISHI[1], NAKASHI SASANO[1], KENTARO YAMAMOTO[1], TSUYOSHI ONOE[1,2], KIYOSHI YODA[3] & KUNI OHTOMO[1]

[1]*Department of Radiology, University of Tokyo Hospital, Tokyo, Japan,* [2]*Department of Radiation Oncology, Cancer Institute Hospital, Tokyo, Japan and* [3]*Elekta, KK, Kobe, Japan.*

To the Editor

The latest linear accelerator equipped with a kilovoltage (kV) cone-beam CT (CBCT) unit is useful for registration at the time of treatment, and thus reduces the setup error [1–4]. But in the case of intracranial or abdominal tumors, the contours of the tumors are difficult to determine on the CT images without contrast media, since such tumors are located next to normal soft tissue whose Hounsfield unit is close to those of the tumors themselves.

Image registration by CBCT is performed based on the bony structures or soft tissue around the tumor. But this process does not necessarily guarantee that the position of the isocenter at treatment is identical with that at the time of planning CT, since bone or soft-tissue registration is based on a volume-matching process. It is difficult to know the exact tumor location for a low-contrast tumor even if on-board registration of the tumor is intended, since the tumor contour is not well visualized even on planning CT images without contrast media. We attempted to visualize metastatic brain

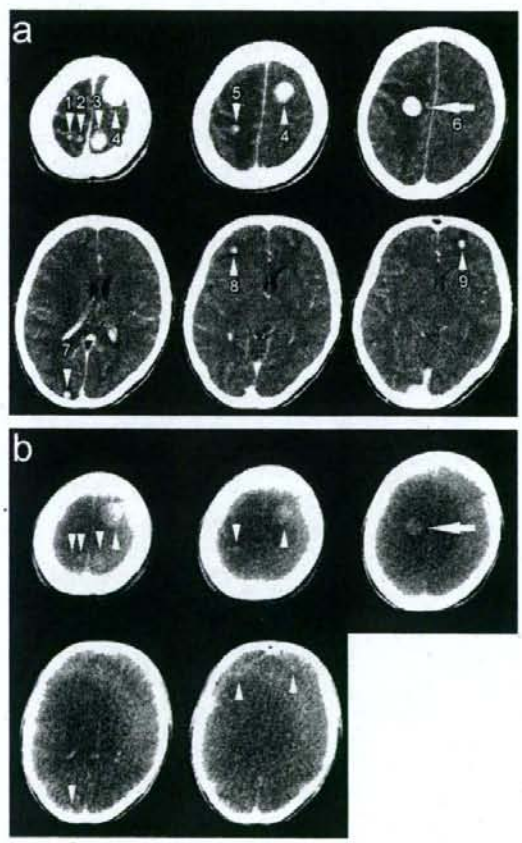

Figure 1 (*Continued*)

Figure 1. Brain tumor images acquired by planning CT (a) and kV CBCT (b) after each intravenous bolus administration of iodized contrast media. The treatment isocenter was set within the tumor indicated by the arrow. Tumors are indicated by the arrowhead. All tumors 6 mm or more in the greatest dimension in the planning CT (a) were also detectable in the CBCT (b). The numbers assigned in the tumor correspond to those in Table I.

Correspondence: Keiichi Nakagawa, Department of Radiology, University of Tokyo Hospital, 7-3-1 Hongo, Bunkyo-ku, Tokyo, 113-8655, Japan. Tel: +81 3 5800 8666. Fax: +81 3 5800 8786. E-mail: k-nak@fg7.so-net.ne.jp

(Received 6 June 2008; accepted 30 June 2008)

ISSN 0284-186X print/ISSN 1651-226X online
DOI: 10.1080/02841860802310983

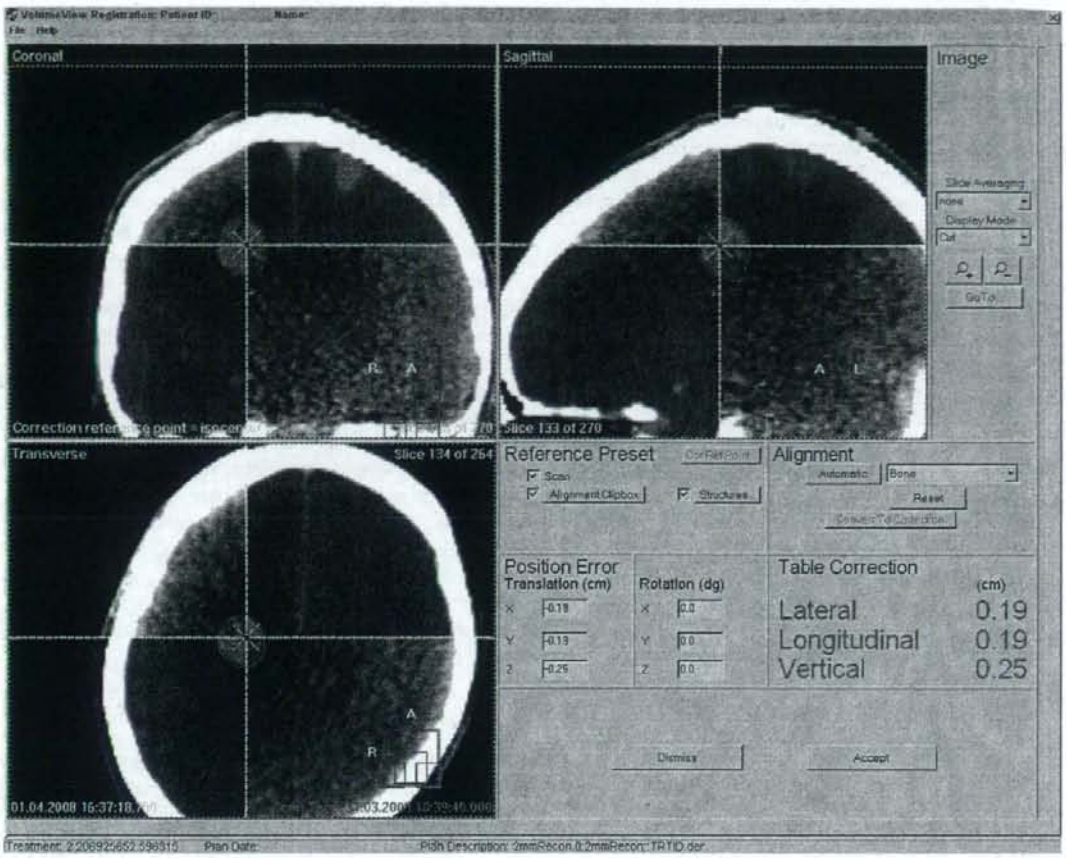

Figure 2. The desktop screen at the time of image registration. After bone registration, the location of the tumor at the isocenter was verified by eye and registered well.

tumors by contrast media administration in kV CBCT images.

A 41-year-old female developed multiple brain metastases from a follicular variant of papillary carcinoma of the thyroid. Radiotherapy planning was performed by Pinnacle[3] (Philips/ADAC, Milpitas, CA) based on CT images acquired by a large-bore CT (Aquilion/LB, Toshiba, Tokyo, Japan) after an intravenous bolus injection of 100 ml of iodized contrast media, Iopamiron 300 (Schering, Berlin,

Table I. Characteristics of the tumors observed in the planning CT.

Tumor No.[1]	Size (mm)[2]	Locus	Possible factors interfering with detectability in CBCT [8]
1	6×4	Rt. high frontal	Cupping artifacts Ring artifact
2	7×5	Rt. high frontal	Cupping artifacts Ring artifact
3	18×16	Lt. high frontal	Cupping artifacts Ring artifact
4	27×19	Lt. high frontal	Cupping artifacts Ring artifact
5	7×7	Rt. high frontal	Cupping artifacts
6	19×16	Rt. frontal	–
7	8×8	Rt. occipital	Cupping artifacts
8	7×7	Rt. frontal tip	Ring artifact
9	8×8	Lt. frontal tip	Ring artifact
10	4×4	Lt. frontal	Cupping artifacts Ring artifact

[1]The numbers of the tumors correnspond to those in Figure 1.
[2]Sizes were measured on 5-mm-thick images of the planning CT.
The greatest dimension and its orthogonal dimension in the axial slice was presented.

Germany). Elekta Synergy (Elekta, Crawley, England), equipped with kV CBCT unit, was used for registration and treatment. Immediately before the treatment, on-board CBCT images were taken four minutes after another intravenous bolus injection of 100 ml of Iopamiron 300. The initial estimation of the tumor registration was performed by built-in bone-matching software because it was very quick. Subsequently, the tumor position in the CBCT image and the isocenter imported from the treatment planning system were displayed for further manual adjustment by eye. Written informed consent on these procedures and treatment was obtained from the patient.

Figure 1a presents representative axial images of the planning CT of this patient. Figure 1b shows kV CBCT images of the corresponding slices taken immediately before the treatment. The isocenter was set within the tumor in the right frontal lobe indicated by the arrow in the Figure 1a. No further manual adjustment was performed after bone matching in this study. The tumor position was directly registered (Figure 2). Thus, it was shown that direct tumor registration was feasible by contrast media-assisted kV CBCT. The patient was treated with whole-brain irradiation.

All the tumors with diameters of 6 mm or more in the greatest dimension observed in the 5-mm-thickness planning CT image were also visible by CBCT (Table I). Ring artifacts of the concentric circle that centers on the treatment isocenter, possibly due to the skull, were seen in the CBCT images (Figure 1b). But these artifacts did not degrade the accuracy of visual verification insofar as the tumor was detectable. Other smaller metastases sized less than 6 mm in the planning CT were undetectable in the CBCT images.

This is the first report of direct tumor visualization and registration in the linear accelerator-mounted CBCT by contrast media administration. It had been reported that sufficient soft-tissue contrast could not be obtained in kV CBCT images by contrast media administration [5]. This is an obstacle for direct tumor registration. To overcome this difficulty, Guckenberger et al. used mobile in-room CT with contrast media just before the treatment [5,6]. The idea of their report is interesting, but the tumor image obtained by in-room CT does not warrant exact tumor position during the treatment. Through our procedure, we can know the exact position of the small tumor itself in an organ with soft-tissue density on-board even during the treatment by simultaneous dual exposure of kV x-ray for CBCT and megavoltage x-ray for treatment [4]. In addition, we determined the minimum size of brain tumors that can be visualized by kV CBCT in this study.

Metastatic brain tumors 6mm or more in the greatest dimension were visualized in the CBCT. This means that tumors 6 mm or more in the greatest dimension are candidates for direct tumor registration by contrast media-assisted kV CBCT. The possible reasons why smaller tumors could not be detected in the CBCT were low contrast of the image, low resolution of the image, the ring artifacts described above, and artifacts due to beam hardening. Most of them had been pointed out previously [7,8], and some problems have already overcome by improvement of the systems [7].

The tumors of the patient involved in this report were strongly and homogeneously enhanced by contrast media. Such characteristics of the tumor appeared suitable for this procedure of visualization. In our preliminary experience, soft-tissue contrast of cystic tumors or heterogeneously enhanced tumors was insufficient in the CBCT images. It is expected that the radiological characteristics of the tumor influence the minimum size of the tumor that can be visualized by CBCT. In the future, we should clarify such relationships by further studies incorporating more patients.

Conflict of Interest Statement

Dr. Nakagawa receives research funding from Elekta K.K. All other authors have no financial or personal relationship with other people or organizations that could inappropriately influence this work.

References

[1] Oldham M, Letourneau D, Watt L, Hugo G, Yan D, Lockman D, et al. Cone-beam-CT guided radiation therapy: A model for on-line application. Radiother Oncol 2005;75: 271–8.

[2] Boda-Heggemann J, Walter C, Rahn A, Wertz H, Loeb I, Lohr F, et al. Repositioning accuracy of two different mask systems-3D revisited: Comparison using true 3D/3D matching with cone-beam CT. Int J Radiat Oncol Biol Phys 2006; 66:1568–75.

[3] Thilmann C, Nill S, Tucking T, Hoss A, Hesse B, Dietrich L, et al. Correction of patient positioning errors based on in-line cone beam CTs: Clinical implementation and first experiences. Radiat Oncol 2006;1:16.

[4] Nakagawa K, Yamashita H, Shiraishi K, Igaki H, Terahara A, Nakamura N, et al. Verification of in-treatment tumor position using kilovoltage cone-beam computed tomography: A preliminary study. Int J Radiat Oncol Biol Phys 2007;69: 970–3.

[5] Guckenberger M, Baier K, Guenther I, Richter A, Wilbert J, Sauer O, et al. Reliability of the bony anatomy in image-guided stereotactic radiotherapy of brain metastases. Int J Radiat Oncol Biol Phys 2007;69:294–301.

[6] Guckenberger M, Sweeney RA, Wilbert J, Krieger T, Richter A, Baier K, et al. Image-guided radiotherapy for liver cancer using respiratory-correlated computed tomography and cone-

beam computed tomography. Int J Radiat Oncol Biol Phys 2008;71:297–304.
[7] Letourneau D, Wong JW, Oldham M, Gulam M, Watt L, Jaffray DA, et al. Cone-beam-CT guided radiation therapy: Technical implementation. Radiother Oncol 2005;75:279–86.
[8] Barrett JF, Keat N. Artifacts in CT: Recognition and avoidance. Radiographics 2004;24:1679–91.

Small cell carcinoma of unknown primary presenting with disease confined to the central nervous system

FIONA CHIONH, ARUN AZAD & CHOOI LEE

Andrew Love Cancer Centre, Barwon Health, Geelong Hospital

To the Editor

We refer to an article published recently in your journal [1], in which the authors stated that extrapulmonary small cell carcinoma (EPSCC) "has been recognized at all sites of the body except the central nervous system". We disagree with this statement and find it ambiguous. If the authors are referring to EPSCC with brain metastases, we argue that this in fact has been widely described [2–9].

Small cell carcinoma of unknown primary (SCUP) is a subset of EPSCC, constituting between 8% [10] to 31% [11] of all EPSCC diagnoses. If the authors are referring to SCUP presenting with central nervous system (CNS) disease, although rare, we have identified one previously reported case in the literature [10]. Furthermore, our institution has recently treated two patients with SCUP who presented with disease isolated to the CNS and who also experienced relapse in the CNS alone.

Both patients were previous smokers, the first a 56-year-old male and the second a 71-year-old female. Both initially presented with a solitary intracranial lesion that was resected. Histology was consistent with small cell carcinoma, and no other sites of disease were found on staging investigations (computed tomography of the chest, abdomen and pelvis and whole body bone scan). Both patients received whole brain radiotherapy (30 Gy in 10 fractions). After 16 and 21 months respectively, both patients relapsed with isolated spinal intradural extramedullary disease that was surgically debulked. Histology was again consistent with small cell carcinoma. Both patients received radiotherapy to the involved spine (30 Gy in 10 fractions), followed by carboplatin (AUC 5, Day 1) and etoposide (120mg/m^2 Days 1–3) chemotherapy. The first patient completed four cycles and remains alive and well 33 months after the initial diagnosis. The second patient developed pneumonia and an acute myocardial infarction after cycle 1, and died shortly thereafter (24 months after the initial diagnosis). In a recent retrospective study, median survival for SCUP was only 2.5 months [11]. By comparison, our patients experienced prolonged disease-free and overall survival.

In summary, not only does EPSCC metastasise to the brain, but SCUP can also present initially in the CNS as demonstrated by the two cases we have described.

References

[1] Lee SS, Lee JL, Ryu MH, Chang HM, Kim TW, Kim WK, et al. Extrapulmonary small cell carcinoma: Single center experience with 61 patients. Acta Oncol 2007;46:846–51.
[2] Cicin I, Karagol H, Uzunoglu S, Uygun K, Usta U, Kocak Z, et al. Extrapulmonary small-cell carcinoma compared with small-cell lung carcinoma: A retrospective single-center study. Cancer 2007;110:1068–75.
[3] Saeki H, Anegawa G, Masuda T, Ohta R, Honda M, Kai T, et al. A case of inoperable gastric small cell carcinoma effectively treated by chemotherapy and radiotherapy (Japanese). Gan To Kagaku Ryoho 2006;33:977–9.
[4] Koide N, Hiraguri M, Kishimoto K, Nakamura T, Adachi W, Miyabayashi H, et al. Small cell carcinoma of the esophagus with reference to alternating multiagent chemotherapy: Report of two cases. Surg Today 2003;33:294–8.
[5] Shamelian SO, Nortier JW. Extrapulmonary small-cell carcinoma: Report of three cases and update of therapy and prognosis. Neth J Med 2000;56:51–5.
[6] Orhan B, Yalçin S, Evrensel T, Yerci O, Manavoğlu O. Successful treatment of cranial metastases of extrapulmon-

Correspondence: Fiona Chionh, Medical Oncology Unit, Level 6 HSB, Austin Hospital, 145 – 163 Studley Road, Heidelberg, Victoria 3084, Australia

(Received 28 May 2008; accepted 30 June 2008)

ISSN 0284-186X print/ISSN 1651-226X online
DOI: 10.1080/02841860802311817

ary small cell carcinoma with chemotherapy alone. Med Oncol 1998;15:66–9.

[7] Khansur TK, Routh A, Mihas TA, Underwood JA, Smith GF, Mihas AA. Syndrome of inappropriate ADH secretion and diplopia: Oat cell (small cell) rectal carcinoma metastatic to the central nervous system. Am J Gastroenterol 1995;90:1173–4.

[8] Zachariah B, Casey L, Zachariah SB, Baekey P, Greenberg HM. Case report: Brain metastasis from primary small cell carcinoma of the prostate. Am J Med Sci 1994;308:177–9.

[9] Hussein AM, Feun LG, Sridhar KS, Otrakji CL, Garcia-Moore M, Benedetto P. Small cell carcinoma of the large intestine presenting as central nervous systems signs and symptoms. Two case reports with literature review. J Neurooncol 1990;8:269–74.

[10] Galanis E, Frytak S, Lloyd RV. Extrapulmonary small cell carcinoma. Cancer 1997;79:1729–36.

[11] Haider K, Shahid RK, Finch D, Sami A, Ahmad I, Yadav S, et al. Extrapulmonary small cell cancer: A Canadian province's experience. Cancer 2006;107:2262–9.

Radiat Med (2008) 26:570–572
DOI 10.1007/s11604-008-0275-2

LETTER TO THE EDITOR

Contrast medium-assisted stereotactic image-guided radiotherapy using kilovoltage cone-beam computed tomography

Keiichi Nakagawa · Hideomi Yamashita · Hiroshi Igaki
Atsuro Terahara · Kenshiro Shiraishi · Kiyoshi Yoda

Received: July 23, 2008 / Accepted: August 19, 2008

Iodized contrast media have been widely used to detect tumors such as brain metastases and hepatocellular carcinomas.[1,2] When patients with such tumors are treated by stereotactic radiotherapy, a major issue is tumor registration at the time of treatment. Because the latest radiotherapy machines are equipped with kilovoltage cone-beam computed tomography (kV CBCT) units,[3] it may be possible to detect normally invisible tumors by contrast medium administration immediately before stereotactic treatment. We have therefore investigated the feasibility of kV CBCT-based direct tumor registration for the two types of tumors mentioned above after contrast medium administration.

Iodized oil (Lipiodol) 3.5 ml was administered via the left hepatic artery under fluoroscopic monitoring. Radiotherapy planning was performed 3 days after the iodized oil administration by Pinnacle (Philips Medical Systems, Eindhoven, The Netherlands) based on CT images taken by a large-bore CT (Aquilion/LB; Toshiba Medical Systems, Tokyo, Japan). Elekta Synergy (Elekta, Crawley, UK) was used for radiotherapy 4 days after the iodized oil administration, with the on-board CBCT image obtained immediately before treatment. The Elekta Stereotactic Body Frame was used for body immobilization.

K. Nakagawa (✉) · H. Yamashita · H. Igaki · A. Terahara · K. Shiraishi
Department of Radiology, University of Tokyo Hospital, 7-3-1 Hongo, Bunkyo-ku, Tokyo 113-8655, Japan
Tel. +81-3-5800-9002; Fax +81-3-5800-8786
e-mail: k-nak@fg7.so-net.ne.jp

K. Yoda
Elekta KK, Kobe, Japan

The initial attempt at tumor registration was performed by built-in bone-matching software because of its quick calculation. In other words, tumor registration was performed using bone anatomy with the assumption that the spatial relation between the bone anatomy and the tumor remained the same at the planning and treatment times. Subsequently, the tumor position in the CBCT image and the isocenter imported from the treatment planning system were displayed for further manual adjustment. The contrast-enhanced tumor position was also verified during treatment by employing a previously reported in-treatment CBCT procedure.[4] All the CBCT images shown in this article were acquired with standard parameters provided by the manufacturer; in other words, we did not increase X-ray dose for this study.

Figure 1a depicts an axial planning CT image of the patient with hepatocellular carcinoma. Figure 1b shows a kV CBCT image after the above-mentioned bone-matching registration, which was performed immediately before treatment. The crossed lines indicate the isocenter position. In this case, no further manual adjustment was required. Although significant ring artifacts were observed possibly due to breathing, it was shown that the artifact did not degrade the accuracy of visual verification. It was also confirmed that the tumor remained in the same position during (Fig. 1c) and immediately after (Fig. 1d) treatment.

Figure 1e shows a brain metastasis image acquired by the planning CT, and Fig. 1f depicts a kV CBCT image after each intravenous bolus administration of iodized contrast medium (Iopamiron 300, 100 ml; Schering, Germany). The planning CT image (2-mm slice) was acquired immediately after the first administration on a treatment planning day, and the CBCT image (converted to a 5-mm slice) was obtained 2 min after the second